Tropical Natural History 15(2): 97–115, October 2015

Embryology of *Spathoglottis plicata* Blume: A Reinvestigation and Additional Data

NARASAK SRIYOT[1], ACHRA THAMMATHAWORN[2] AND PIYADA THEERAKULPISUT[1*]

[1] *Applied Taxonomic Research Center, and Salt-tolerant Rice Research Group, Department of Biology, Faculty of Science, Khon Kaen University, Khon Kaen 40002, THAILAND*
[2] *Office of General Education, Khon Kaen University, Khon Kaen 40002, THAILAND*
* Corresponding author. Piyada Theerakulpisut (piythe@kku.ac.th)
Received: 16 May 2015; Accepted: 6 September 2015

ABSTRACT.– *Spathoglottis plicata* Blume is very popular among terrestrial orchids because it is attractive, easy to grow and can flower all year round. The aim of this study was to reinvestigate the embryological characters using classical paraffin embedding and sectioning, along with ovule clearing and scanning electron microscopy analyses. The simultaneous cytokinesis results in decussate, isobilateral, linear, T-shaped and tetrahedral microspore tetrads. Mature pollen grains are two-celled with perforate sculpturing. The anther wall is comprised of an epidermis, two to three layers of endothecium, one layer each of middle layer and one layer of binucleate glandular tapetal cells. At anthesis, the mature anther wall is composed of epidermis and fibrous endothecium. At 9 d after pollination (DAP), the mature ovules are anatropous, bitegmic and tenuinucellate. The megaspore tetrad is linear. Development of the embryo sac conformed to the *Polygonum* type. The pollen tube enters the embryo sac through the micropyle (porogamy), and double fertilization is observed at 15 DAP. The zygote divides transversely to form a two-celled proembryo. The basal cell becomes the suspensor initial cell, whereas the terminal cell divides transversely to form a linear three-celled proembryo. The proembryonal tetrad is T-shaped. Embryogenesis is of the *Onagrad* type. The suspensor is single-celled, hypertrophied and cap-, globular- or sac-like. Fruit opens at 30 DAP. Seeds are fusiform in shape with longitudinally oriented testa cells with a smooth periclinal seed surface and straight anticlinal walls. The mature globular embryo is acotyledonous and lacks differentiation. Furthermore, cleavage polyembryony gives rise to twin embryos.

KEY WORDS: *Spathoglottis plicata*, ground orchid, embryology, Orchidaceae

INTRODUCTION

The genus *Spathoglottis* Blume is a member of the subfamily Epidendroideae. All members of this genus are terrestrial and most grow at low to moderate altitudes, although a few taxa occur at high altitudes in grasslands and open forests in moist areas (Dressler, 1993; Beltrame, 2006). This genus is composed of 10 species distributed from Sri Lanka, India and the Andaman Islands through Indochina to southern China, Malaysia and Indonesia east to the Philippines, New Guinea, Australia and the Pacific islands as far as Samoa (Seidenfaden & Wood, 1992). In Thailand, five species have been recorded (Seidenfaden, 1986).

Orchidaceae is of interest for embryological studies because of the diversity in the development and organization of the female gametophyte, characteristics of suspensor and different patterns of polyembryony (Sood, 1985).

The ground orchid (*Spathoglottis plicata*) is one of the most commonly cultivated orchids in Southeast Asia and could be found in gardens throughout the region. It is suitable as a potted orchid because it is very attractive, fast growing, easy to grow and with rapid fruit

maturation. At maturity, plants flower almost throughout the year (Kheawwongjun & Thammasiri, 2008). These attributes have also led to it being used as a model for orchid studies. This taxon has already been studied in many aspects, including artificial propagation (Teng et al., 1997; Minea et al., 2004; Sinha et al., 2009; Thakur & Dongarwar, 2012; Aewsakul et al., 2013; Sebastinraj & Muhirkuzhali, 2014), cytology (Ramesh & Ranganathan, 2008), physiology (Wang et al., 2002, 2003; Novak & Whitehouse, 2013), pollination biology (Soguillon & Rosario, 2007; Thakur & Dongarwar, 2012) and molecular biology (Ranghavan & Goh, 1994; Yang & Loh, 2004).

The embryology of *S. plicata* has been examined by a few authors, where the work of Swamy (1943a, 1949a,b), Prakash & Lee-Lee (1973), Veyret (1974) and Ansari (1977) have detailed aspects of the sporogenesis, gametogenesis and embryogenesis, but the information is rather fragmentary. In addition, these researches were documented only by line drawings and have not been reinvestigated so far. The aim of this study was to reinvestigate the microsporogenesis and microgametogenesis of *S. plicata* in relation to the floral developmental stages using the classical paraffin embedded serial section analysis, as well as the post-pollination development of megasporogenesis, megagametogenesis and embryogenesis using ovule clearing and scanning electron microscopy (SEM) analyses. The data presented here will provide valuable background knowledge for both conservation and molecular biology studies of this species.

MATERIALS AND METHODS

Plant Materials

The samples of *S. plicata* (Ground orchid) were grown in the greenhouse at the Department of Biology, Faculty of Science, Khon Kaen University. The ground orchid (Fig. 1A) is a perennial plant with ovoid pseudobulbs covered with fibrous leaf bases. There are 4–8 linear-lanceolate leaves per pseudobulb, each up to 35 cm long and 2–6 cm wide, yellow-green to dark-green and with prominent veins abaxially. The inflorescences are lateral racemes, up to 25–130 cm long, bearing many successive and loosely spaced flowers. Flowering can occur from August to March, the peak period being November to February.

Microsporogenesis, Microgametogenesis and Anther Wall Anatomy

The floral buds and blooming flowers (Fig. 1B) were harvested at different stages of development, during the flowering period (November 2013–March 2014). The length of each floral buds was measured from the tip to the base of the perianth, and they were divided into different stages based on their length and fixed in 70% (v/v) FAA (1:1:18 (v/v/v) ratio of formalin: acetic acid: 70% (v/v) ethanol). Dehydration, infiltration and embedding were performed in the conventional way. Sections were cut at 5 µm thick with a steel knife on a sliding microtome. They were stained with safranin and fast-green combination, then mounted in DePeX mountant (Thammathaworn, 1995) and observed by light microscopy. The anther squash was also prepared and stained with 1% (w/v) aceto-orcein to clarify the mitotic division of microspore nuclei.

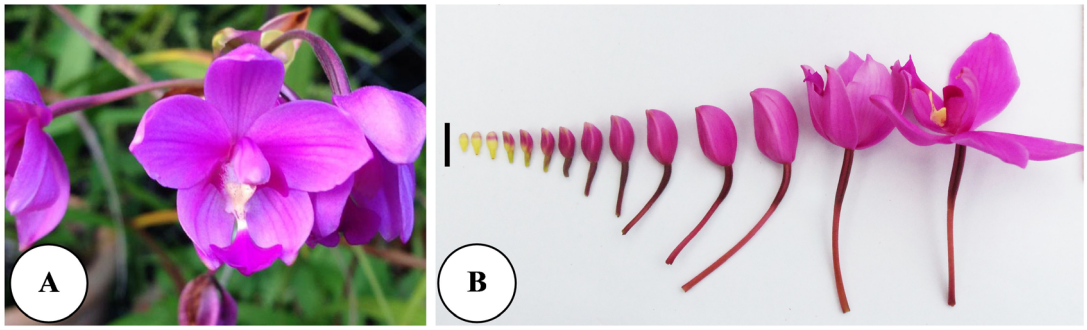

FIGURE 1. Flower morphology of *S. plicata*. A. The front view of a blooming flower. B. Flowers at different stages of development were prepared for anther transverse sections with paraffin method. Scale bar = 1 cm.

To study the pollinium morphology and the pollen grain surface features, the pollen grains were fixed in 70% (v/v) FAA and then transferred to 70% (v/v) alcohol. To preserve the exine, no acetolysis was performed. Dehydration was performed in a series of increasing % (v/v) acetone. Specimens were then critical point dried using CO_2, placed on specimen stubs with double sided silver tape and sputter coated with gold. The samples were examined under SEM (Philips, XL-20) at the Institute of Botany, Faculty of Biology, University of Innsbruck, Austria. Pollen terminology followed that defined by Punt et al. (2007).

Megasporogenesis, Megagametogenesis and Embryogenesis

One of the unique characters of ovule development in Orchidaceae is that ovules normally do not appear at the time of anthesis. The development of ovules is activated by pollination and normally takes several weeks to complete (Swamy, 1949a, 1949b). In order to ensure a good fruit set, the stigma receptivity of the flower at anthesis was tested using hydrogen peroxide, where the appearance of bubbles could be observed on receptive stigma (Dafni & Maués, 1998). Flowers at similar stage were then artificially self-pollinated. To this end the anther cap and pollinia were gently removed by a toothpick. The pollinia were displaced from the column by applying a slight upward pressure to the bottom of the anther cap and the pollinia adhered to the toothpick on contact. After removal, the pollinia were transferred to the same flower by placing them onto the stigmatic surface (Kauth et al., 2008). The efficiency of pollination was checked by flower senescence and fruit development. The resulting fruits at different stages of development were chosen at intervals of 3 d. Approximately 30 developing fruits were chosen and fixed in 50% (v/v) FAA. The ovules were carefully removed to a slide with a few drops of Herr's 4 ½ clearing solution (Herr, 1971), no dehydration was necessary, and a cover glass was then added. Herr's clearing solution made the samples transparent in a couple of minutes. Photographs were captured under Nomarski illumination using an Olympus BX51 microscope coupled to an Olympus DP11 digital camera.

In order to study the morphological characters of the seed coat, seeds at the fruit dehiscence stage were prepared for SEM analysis as described above. Measurements were performed on the width and length of the embryos and seeds using a minimum of 15 seeds.

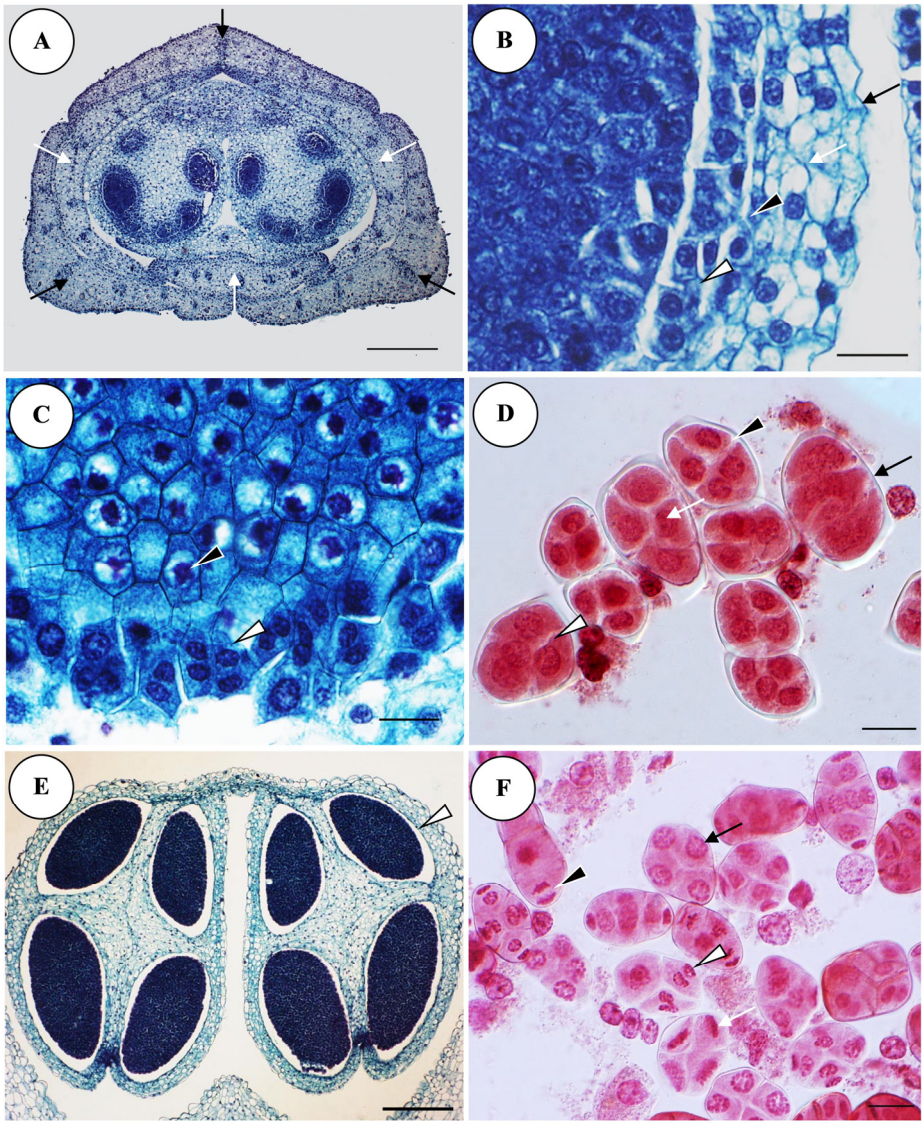

FIGURE 2. Anther anatomy, microsporogenesis and microgametogenesis. A. Transverse section of a young floral bud showing two rows of perianth. The outer row has three sepals (black arrows) and the inner one has three petals (white arrows) with a young anther in the center. B. Portion of a transverse section of a fully formed anther showing the epidermis (black arrow), 2–3 layers of endothecium (white arrow), middle layer (black arrowhead) and tapetum (white arrowhead). C. Portion of a transverse section of an anther showing the binucleate glandular tapetal cell (white arrowhead) and microspore mother cell (black arrowhead). D. Linear (black arrow), isobilateral (black arrowhead), decussate (white arrow) and tetrahedral (white arrowhead) microspore tetrads. E. Transverse section of an anther at an advanced stage of development showing two thecae with eight microsporangia. The degeneration of the middle layer and tapetum results in the separation of the developing pollinia from the anther wall (arrowhead). F. Stages of mitosis in microspores: prophase (black arrow), metaphase (white arrow), anaphase (black arrowhead) and telophase (white arrowhead). Scale bars: A, E = 300 µm; B–D, F = 20 µm.

RESULTS

Microsporogenesis, Microgametogenesis and Anther Wall Anatomy

A transverse section of the young floral bud revealed two rows of perianth. The outer row had three sepals and the inner row had three petals. The third petal was modified into a labellum or lip and was commonly found oriented towards the bottom of the young floral bud. A transverse section of the young anther showed two thecae that were oriented towards the labellum. In each theca, a complete septum of sterile cells (parenchyma cells) was formed and divided each theca into four microsporangia. Therefore, an anther was composed of eight microsporangia (Fig. 2A).

In order to facilitate description, the pollinium development was categorized into four developmental stages, described as follows.

Stage 1: Microspore mother cell (flowers 3–4 mm long) At the early stage, the microspore mother cells were compactly arranged without any intercellular space. They were either hexagonal or polygonal in outline, possessed dense cytoplasmic contents and prominent nuclei (Fig. 2B). The fully formed anther wall was made up of 5–6 layers: an epidermis, 2–3 layers of endothecium, a middle layer and a layer of tapetum. The tapetum is of the glandular type and its cells were uninucleate (Fig. 2B). Thereafter, the microspore mother cells underwent meiotic division. The nucleolus and nuclear membrane disappear and the tapetal cells become binucleate at the time the microspore mother cells are in synizesis (Fig. 2C). The first meiotic division is not followed by wall formation, and the second meiotic division is accompanied by simultaneous cytokinesis. Callose walls are formed and give rise to a microspore tetrad.

Stage 2: Microspore tetrad (flowers 4.5–5 mm long) Soon after the meiotic division, the microspore tetrads become enclosed in a thick callose wall but do not separate out of the tetrad configuration. The nucleus of the freshly produced microspore occupies a somewhat central position in the cell. Microspore tetrads are decussate, isobilateral, linear, or rarely T-shaped and tetrahedral (Fig. 2D). The anther wall is comprised of an epidermis, 2–3 layers of endothecium, while the middle layer and tapetum gradually degenerate resulting in the separation of the developing pollinia from the anther wall (Fig. 2E).

Stage 3: Early stage of pollen grain (flowers 6–7 mm long) The development of the male gametophyte takes place at the distal poles of the microspores. The microspore slightly enlarges in size and the nucleus migrates to a peripheral position away from the center. The microspore nucleus undergoes mitotic division (Fig. 2F), and the generative cell is normally cut off towards the exterior side of the microspore tetrad. It is characteristically lens-shaped and normally smaller than the vegetative cell. The nucleus of the generative cell reveals a greater avidity for stains than the contents of the vegetative cell. A transitory wall is deposited between the vegetative and generative cells. Thereafter, the wall disappears and its place may be distinguished by a clear space (Fig. 3A). The anther wall consists of an epidermis, 2–3 layers of endothecium, of which one layer develops fibrous thickenings (Fig. 3B), while the middle layer and tapetum continuously degenerate further.

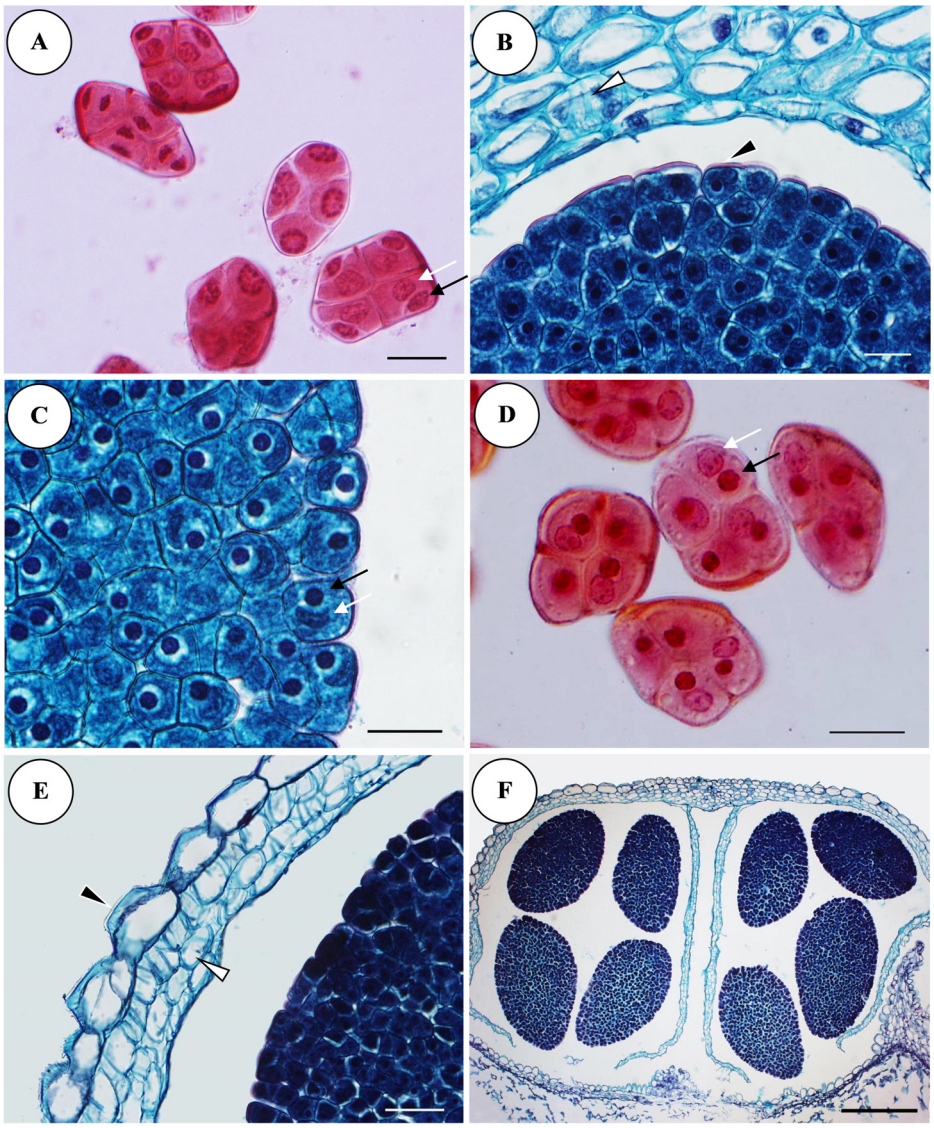

FIGURE 3. Microgametogenesis and anther wall anatomy. A. An early stage of pollen grain development, where microgametogenesis takes place at the distal poles of the microspores showing a generative cell (black arrow) and vegetative cell (white arrow). B. The pollen walls give a red colour when stained with safranin, indicating the present of callose in the wall (black arrowhead). The endothecium develops fibrous thickening (white arrowhead). C. Two-celled pollen grains showing the generative cell (black arrow) and vegetative cell (white arrow). At this stage, the vegetative cell is crescent-shaped. D. Two-celled mature pollen grains showing the generative cell (black arrow) and vegetative cell (white arrow). E. Portion of a transverse section of a mature anther showing the epidermis (black arrowhead) and 2–3 layers of fibrous endothecium (white arrowhead). F. Transverse section of an anther at anthesis showing the eight pollinia. Scale bars: A–D = 20 µm; E = 40 µm; F = 300 µm.

Stage 4: Pollen grain (flowers 8.5–25 mm long). The generative cell detaches itself from the parent wall and migrates into the cytoplasm of the vegetative cell. The

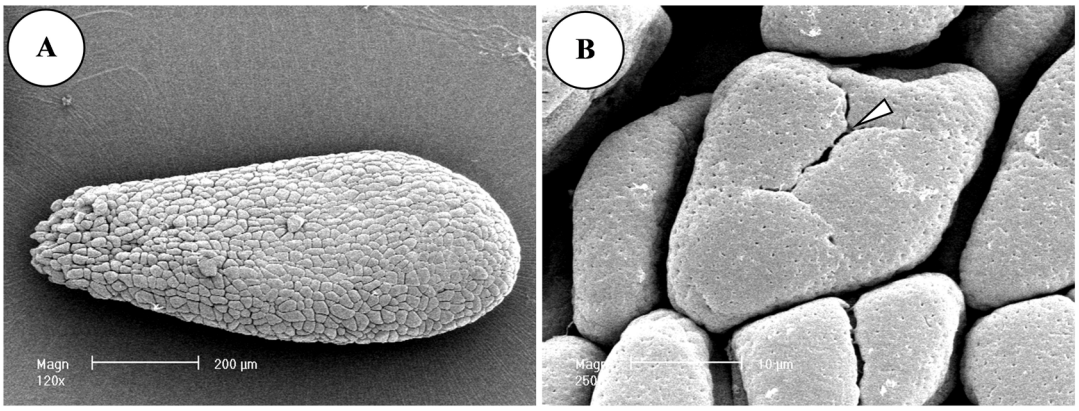

FIGURE 4. Pollinium morphology and the pollen grains surface features. A. A clavate pollinium. B. The decussate pollen grains are tightly packed with perforate sculpturing (arrowhead indicates seam).

nucleus of the vegetative cell becomes semilunar due to the pressure exerted by the generative cell. An empty space could be seen around the generative cell (Fig. 3C). At shedding, the pollen grains are two-celled and consist of a very darkly stained, globose generative cell and a faintly stained, larger vegetative cell (Fig. 3D). The tetrad of pollen grains was enclosed in thick callose walls (Fig. 3B, D). In the mature anther, the wall consists of an epidermis and three layers of fibrous endothecium, while the middle layer and tapetum have completely degenerated (Fig. 3E). The sterile cells of the septum between the four microsporangia in each theca completely disintegrate resulting in eight pollinia per anther (Fig. 3F). The SEM analysis revealed that the pollinium was clavate shaped (Fig. 4A). The mature pollen grains are irregular or polygonal in shape and appear in tightly packed tetrads. The exine sculpturing is perforate (Fig. 4B).

Megasporogenesis and Megagametogenesis

At the time of anthesis, numerous ovular primordia appear from the placental ridges. The ovular primordium possesses an axial row of approximately five to eight nucellar cells enclosed by a layer of epidermal cells (Fig. 5A). The terminal nucellar cell, underneath the epidermis, differentiates into the archesporial cell and is distinguished by its large size, dense cytoplasmic contents and prominent nucleus. The remaining cells below the archesporial cell do not undergo any divisions but persist for a long time, even after fertilization. Mitotic division of the epidermal cell (Fig. 5B) gives rise to a small projection in the epidermal layer of the ovular primordium. This swelling forms the initiation of the inner integument and consists of two enlarged epidermal cells. These cells form the two layers of the inner integument (Fig. 5C, D). The initiation of the outer integument originates in the same way as that of the inner one but occurs beyond the inner integument (Fig. 5E, F). At 9 d after pollination (DAP), the ovules are anatropous, bitegmic and tenuinucellate (Fig. 5G). The inner integument alone forms the micropyle and completely surrounds the nucellus. (Fig. 5H).

The hypodermal archesporial cell enlarges in size and subsequently transforms into the megaspore mother cell, which slightly elongates before undergoing

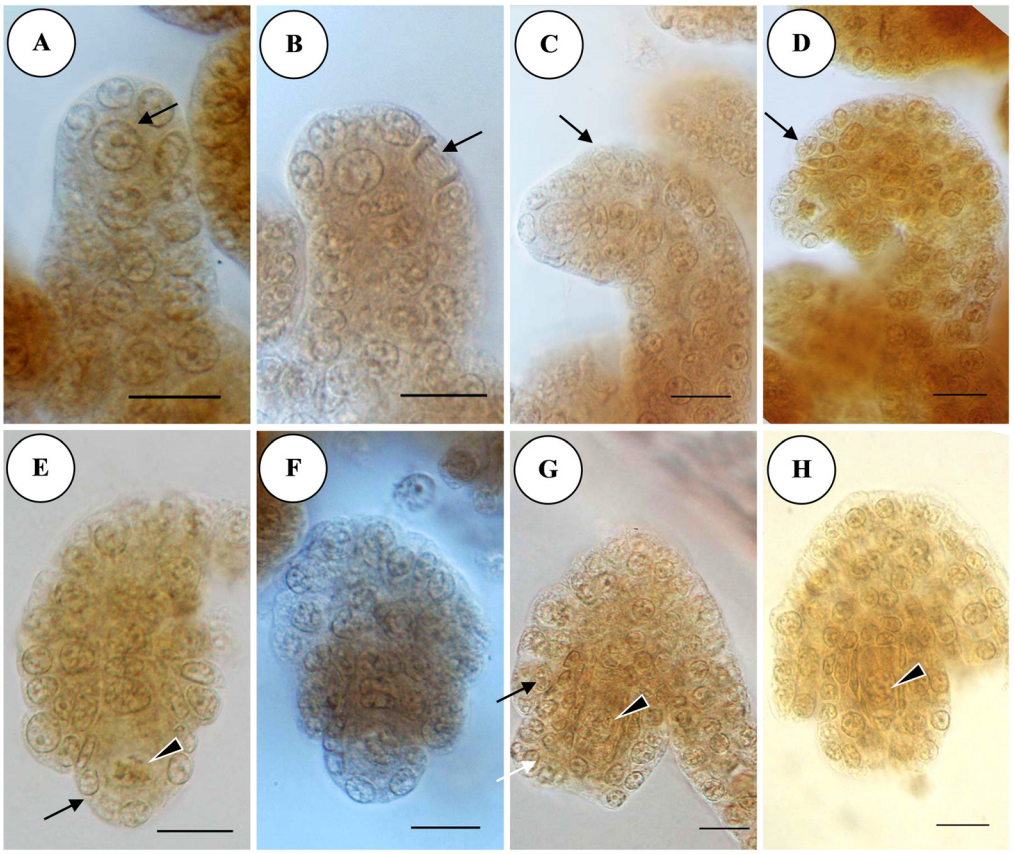

FIGURE 5. Ovule development and megasporogenesis. A. Ovular primordium showing archesporial cell (arrow) at the terminus. B. Anticlinal division (arrow) of the epidermal cell gives rise to the initiation of the inner integument. C. Young ovule showing the dermal origin of the inner integument (arrow). D. Ovule at an advanced stage of development, where the inner integument (arrow) starts to grow. E. Developing ovule showing the megaspore mother cell (arrowhead) encompassed by a single-layer nucellar epidermis (arrow). F. Ovule at an advanced stage of development. G. Mature ovule showing an outer integument (black arrow), inner integument (white arrow) and megaspore mother cell (arrowhead). H. Mature ovule showing the megaspore mother cell (arrowhead) in prophase during the first meiotic division. Scale bars = 20 µm.

meiosis (Fig. 5G). The nucleus is located at the micropylar end of the cell. The first meiotic division results in a dyad of two unequal cells, the micropylar one normally being the smaller (Fig. 6A). The dyad cells undergo a second meiotic division to give rise to four linear megaspores (Fig. 6B). Soon after, the lowermost cell is functional and the rest degenerate (Fig. 6C). The functioning megaspore divides mitotically and gives rise to a binucleate embryo sac. A large vacuole separates the two nuclei (Fig. 6D). Both nuclei divide again to produce a tetranucleate embryo sac (Fig. 6E). By one further division these four nuclei give rise to an eight-nucleate embryo sac organized in the normal pattern. Hence, the mature embryo sac is composed of an egg apparatus, a secondary nucleus and three antipodal cells. The sac is longer than it is broad and is typically ovoid in shape (Fig.

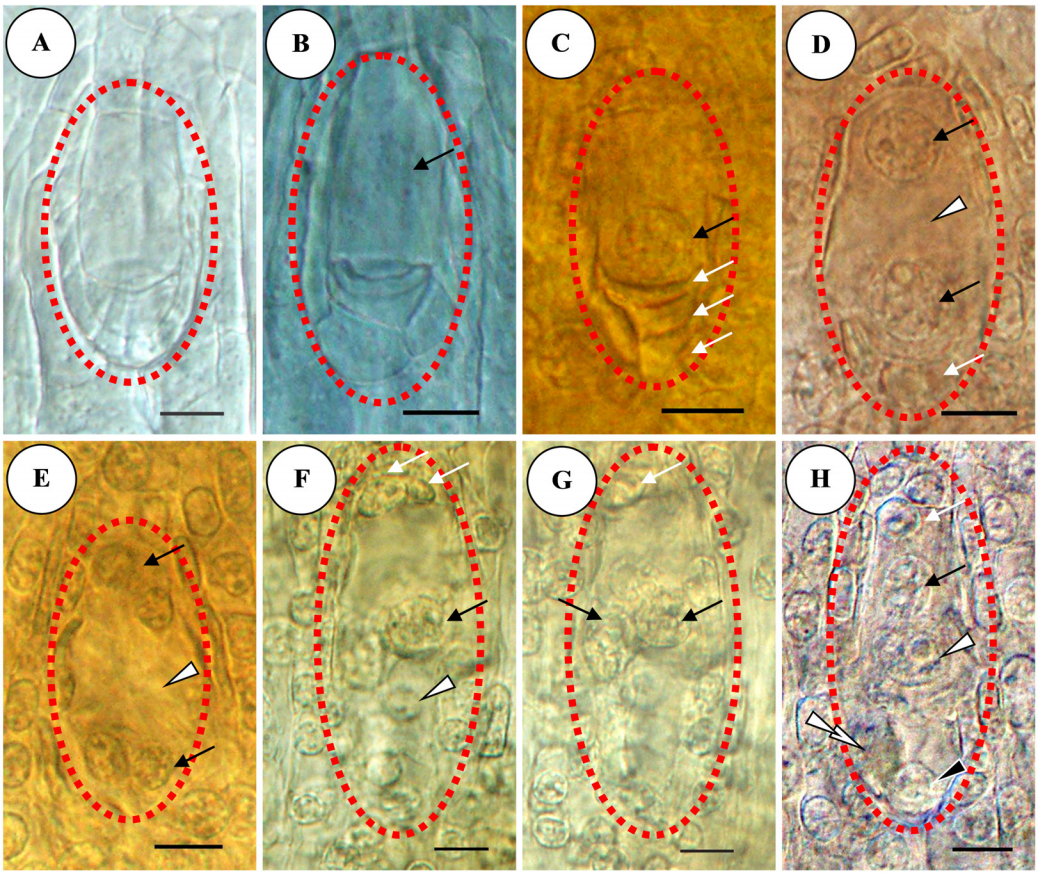

FIGURE 6. Megasporogenesis and megagametogenesis. A. Dyad with unequal cells. B. Linear megaspore tetrads; arrow indicates the lowermost cell. C. Functioning megaspore (black arrow) with three degenerated cells at the micropylar end (white arrows). D. Binucleate embryo sac showing two nuclei (black arrow), three degenerated cells (white arrow) and central vacuole (arrowhead). E. Tetranucleate embryo sac (black arrows) and central vacuole (arrowhead). F. Organized embryo sac showing two antipodal cells (white arrows), polar nucleus (black arrow) and egg cell (arrowhead). G. Mature embryo sac at the same stage as that seen in Fig. 6F (in a different plane) showing two polar nuclei (black arrow) and an antipodal cell (white arrow). H. The embryo sac after double fertilization showing the zygote (white arrowhead), primary endosperm nucleus (black arrow), an antipodal cell (white arrow), synergid (black arrowhead) and pollen tube contents with degenerated synergid (double arrowheads). Scale bars = 10 µm.

6F, G). Female gametophyte development is of the monosporic, *Polygonum* type.

Embryogenesis

At 15 DAP, double fertilization normally occurs and is of the porogamous type. The pollen tube, before it enters the micropyle, is found to grow along the funiculus and the inner integument (Fig. 7A). The tube pierces one of the synergids and releases its content into it. One sperm nucleus fuses with the egg, while the other with the product of the fusion of the polar nuclei to form the primary endosperm nucleus. Triple fusion is completed at the time of syngamy (Fig. 6H). Soon after, the antipodal cells rapidly degenerate at the early stages of embryo development.

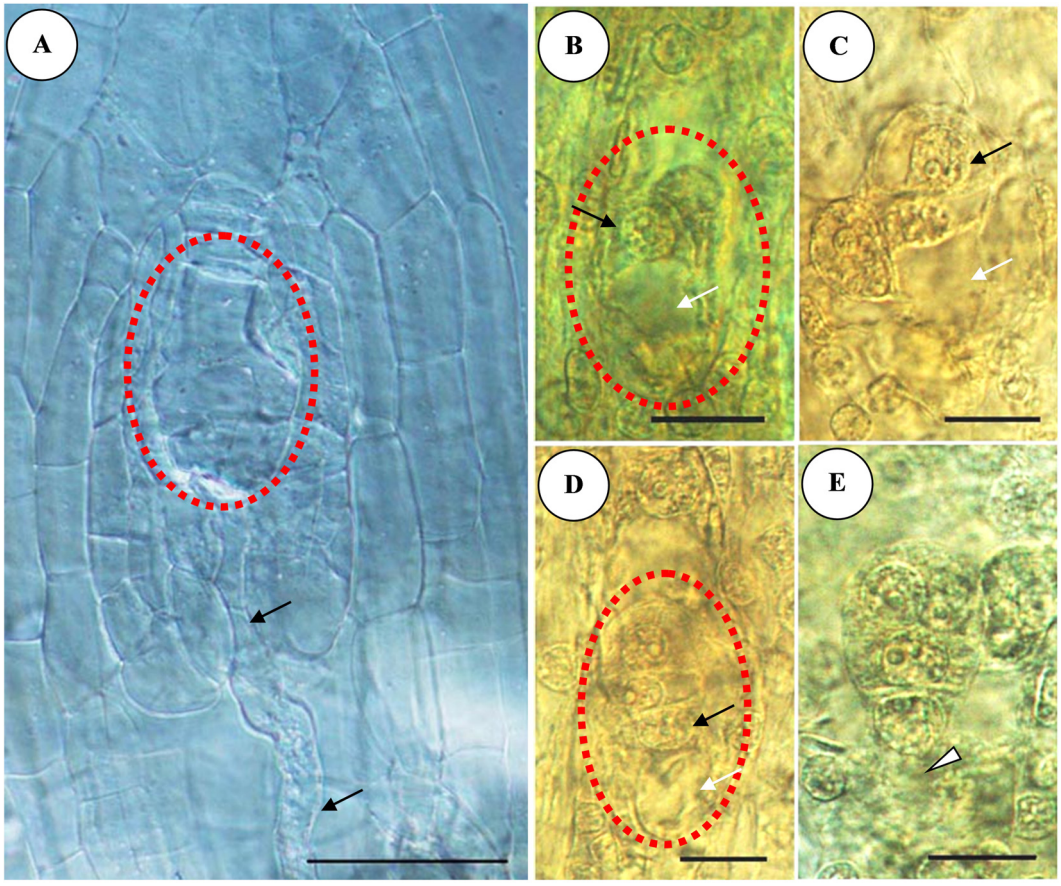

FIGURE 7. Pollen tube and stages in embryo development leading to the formation of globular embryo. A. A pollen tube (arrows) penetrating the micropyle. B. The zygote is polarized with a chalazally located nucleus (black arrow) and a prominent vacuole occupying the micropylar end (white arrow). C. Two-celled proembryo showing the basal cell (white arrow) and terminal cell (black arrow). D. Three-celled proembryo showing the nucleus of the suspensor initial cell (black arrow) and vacuole (white arrow). E. T-shaped proembryonal tetrad. Arrowhead indicates the suspensor cell. Scale bars: A = 40 µm; B–E = 20 µm.

The zygote and proembryo are found within the developing fruits at approximately 18 DAP. The zygote is a highly polarized cell with a chalazally situated nucleus and a prominent vacuole occupying the micropylar region. The cytoplasm of the zygote is confined at the chalazal end (Fig. 7B). The primary endosperm nucleus fails to develop and is eventually absorbed by the proembryo during the early stages of embryo development. The first division of the zygote is transverse and gives rise to a proembryo consisting of a smaller terminal cell (*ca*) and a larger basal cell (*cb*) (Fig. 7C). The former grows out into the embryo sac, whereas the latter remains united to the inner wall near the micropyle. The *cb* cell then divides transversely giving rise to a lower cell (*ci*) and a middle cell (*m*). A row of three-celled proembryos commonly appeared (Fig. 7D). The lowest cell (*ci*) towards the base becomes the suspensor

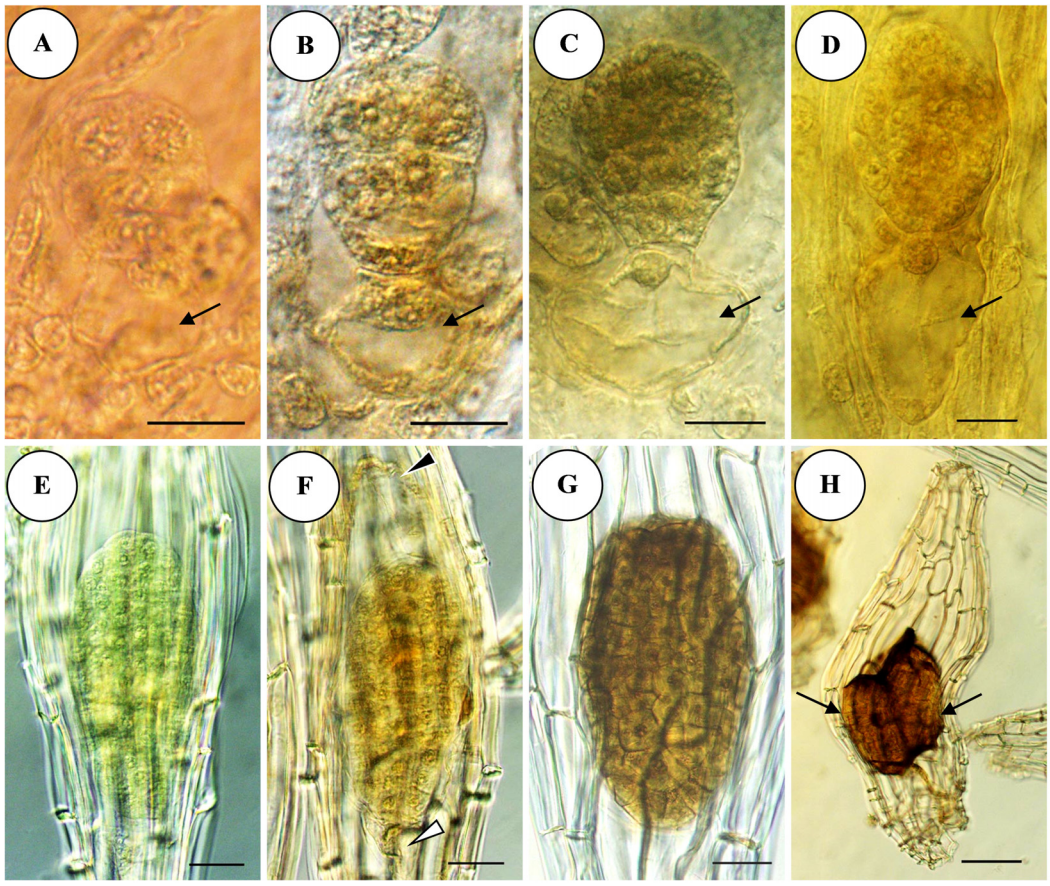

FIGURE 8. Stages in embryo development leading to the formation of the globular embryo and mature seed. A. An advanced stage in embryogenesis. Arrow indicates the suspensor cell. B. Globular embryo with globular suspensor (arrow). C. Globular embryo with cap-like suspensor (arrow). D. Globular embryo with sac-like suspensor (arrow). E. Embryo at an advanced stage of development showing the chlorophyllous embryo. F. The golden yellow embryo. The suspensor degenerates at this stage and only the vestige (white arrowhead) is seen, while the inner integument cells gradually degenerate (black arrowhead). G. Mature globular embryo. The embryo is encapsulated with a sclerified seed coat. H. Polyembryony, arrows indicate twin embryos. Scale bars: A–D = 20 µm; E–G = 40 µm; H = 75 µm.

initial cell with a prominent vacuole located at the micropylar end of the cell. The nucleus and cytoplasm are situated towards the embryo proper. The suspensor initial cell does not undergo any further divisions and directly transforms to the suspensor. Only the *ca* and *m* cells continue to divide and give rise to the embryo proper. The terminal cell divides vertically forming two juxtaposed cells.

The four-celled proembryo corresponds to the A2 category (T-shaped) of Veyret (1974) (Fig. 7E). Afterwards, the cells at the terminus of the proembryonal tetrad are responsible for the formation of the embryo proper. These cells begin to divide and the newly formed cells enlarge in preparation for mitotic divisions, leading to an increased size of the embryo proper (Fig. 8A). The subsequent divisions are irregular and result

TABLE 1. Main developmental stages that occur in developing fruits in relation to the days after pollination (DAP).

DAP	Stages of development
0–6	Archesporial cell
9	Megaspore mother cell
12	Dyad, tetrad, 2–8 nucleate embryo sac
15	Fertilization
18–21	Zygote, proembryo, globular embryo and single-celled suspensor
24–27	Chlorophyllous embryo, golden yellow embryo, suspensor degenerates
30	Mature fruit splits, dark brown globular embryo

in a globular embryo (Fig. 8 B–D). The terminal cell (*ca*) contributes a larger number of cells to the body of the embryo proper than the middle cell (*m*). At the same time, the suspensor cell enlarges to enormous proportions by vacuolation. The suspensor appears globular (Fig. 8B), hood-like (Fig. 8C) or sac-like (Fig. 8D) with a hypertrophied nucleus. However, no branching of the suspensor is found. It is a single cell and fills a large vacuole restricted at the micropylar end, whereas the nucleus is characteristically situated at the constricted region. The suspensor cell is strongly appressed against the embryo proper and constricted at the point of attachment (Fig. 8D).

Throughout embryo development, the suspensor cell is more vacuolated than the cells of the embryo proper. Thereafter, the globular embryo becomes greenish because it contains chlorophyll (chlorophyllous embryo) (Fig. 8E) and at this developmental stage, the cells of the entire inner integument, the inner layer of the outer integument and the suspensor cell begin to collapse as they become dehydrated. Subsequently, the embryo begins to turn golden yellow and the suspensor cell is completely degenerated by this stage with only the vestige being apparent (Fig. 8F). It should be noted that the embryo reached maturity (27 DAP) prior to fruit dehiscence (30 DAP).

At 27 DAP, the embryo proper attains its maximum size and mitotic divisions in the embryo stop. It is yellowish brown and becomes dry and detaches from the placenta. The embryo occupies the central area, conforming to the widest zone of the seed, and is 10 cells long and five cells across at its widest point. An apical meristem and cotyledon are not present. It should be noted that the embryo contains different cell sizes, with the cells towards the terminus being smaller than those towards the micropylar region (Fig. 8G). The cells of the entire inner integument and the inner layer of the outer integument completely degenerate, resulting in a transparent seed coat. Hence, the mature seed coat consisted only of cells derived from the outer integument. Storage product is not present within the testa cells. It must be noted that polyembryony is seen to be of twin embryos only. The two embryos in a seed are normally lying nearly parallel to each other (Fig. 8H). The key embryological events in the ovule and embryo development from anthesis to fruit dehiscence that occur in *S. plicata* are summarized in Table 1.

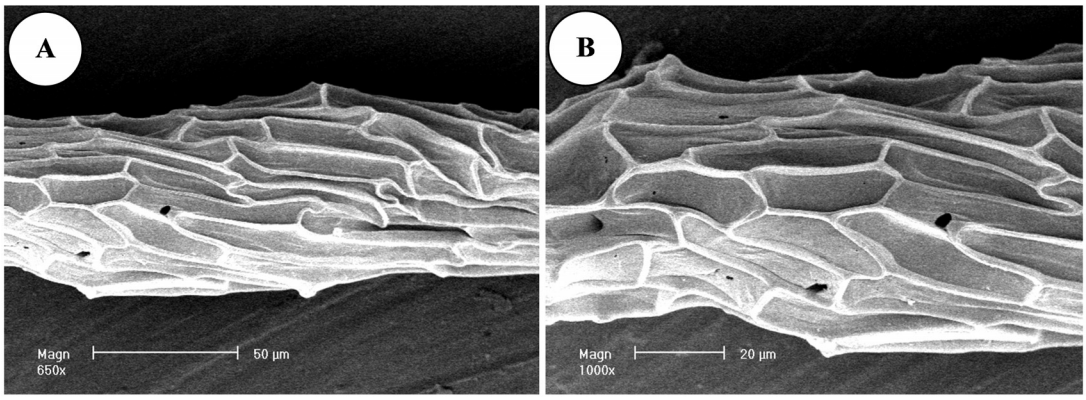

FIGURE 9. Scanning electron micrographs of *S. plicata* seed. A. Seed surface with longitudinally oriented testa cells (650 x magnification; scale bar = 50 µm). B. Portion of the seed showing straight anticlinal and smooth periclinal walls of the testa cells under 1000 x magnification (scale bar = 20 µm).

The micromorphology of the seeds reveals that they are minute, dust-like and fusiform in shape. They are brown and have an aperture in the posterior. The seed length ranges between 100–200 µm and width from 50–100 µm. The testa cells are longitudinally oriented, tetragonal, pentagonal, hexagonal or polygonal in outline. These cells have thick anticlinal walls with a raised anticlinal boundary with no intercellular spaces between them. The periclinal walls are unsculptured (Fig. 9A, B).

DISCUSSION

Although most features in anther development, microsporogenesis and microgametogenesis of *S. plicata* in this study conform to the common characters in Orchidaceae, some characters of interest were noted. Simultaneous cytokinesis is a common character in Orchidaceae (Johri et al., 1992), while successive cytokinesis has been reported in a few taxa (Sood & Rao, 1988; Aybeke, 2012). The present study conforms to the former state. The anther wall, which consists of four layers, is known as the Monocotyledonous type whereas that containing more than four layers is called the Massive type (Sood & Rao, 1988; Kant et al., 2013). From our observation, the fully formed anther wall is composed of 5–6 layers due to the presence of a 1–2 layer thick endothecium, and so it is of the Massive type. In the majority of orchids, the tapetal cells remain uninucleate throughout and are of the glandular type. However, *S. plicata* possesses a binucleate tapetum that has previously only been reported in a few species, including *Paphiopedilum druryi* (Swamy, 1949a), *Epipactis latifolia* (Sood, 1997) and *E. veratrifolia* (Bhanwra et al., 2006). It appears that a binucleate tapetum is limited to primitive orchids and provides extra nutrition to the developing pollen grains (Kant & Bhanwra, 2010). It is important to note that the tapetal cells become binucleate at the time the microspore mother cells are in synizesis.

From the pollen SEM study, the pollinium in *S. plicata* is clavate shaped (Fig. 4A), which is common in Epidendroideae (Freudenstein & Rasmussen, 1996). The sculpturing of the pollen wall is perforate (Fig. 4B). The features, like the sculpturing of exine and the variation in

number and shape of pollens have been used as taxonomic characters in Orchidaceae (Pridgeon, 1999; Kant & Bhanwra, 2010).

The traditional paraffin embedded and serial sectioning method was used in the embryological studies of *S. plicata* by Swamy (1949a, 1949b) and Prakash & Lee-Lee (1973). These techniques are laborious and require analysis of numerous serial specimens, which can often lead to misinterpretation. The ovule clearing technique permits the rapid whole ovule observation without disruption of three-dimensional relationships making it very effective for the observation of thick specimens like developing ovules and embryos (Stelly et al., 1984).

Prakash & Lee-Lee (1973) reported T-shaped tetrad of megaspores in *S. plicata* whereas, in contrast, our finding reveals linear tetrads (Table 2). The occurrence of T-shaped and linear tetrads in the same species has also been reported in *Herminium monorchis* (Fredrikson, 1990) and *Platanthera bifolia* (Fredrikson, 1991).

The ovule development of *S. plicata* conforms to the pattern of Orchidaceae forming an anatropous, bitegmic and tenuinucellate ovule. The development of the female gametophyte is monosporic following the *Polygonum* type with linear or T-shaped megaspore tetrads and eight-nucleate. A mature embryo sac containing eight nuclei appears to be the most common form in Orchidaceae (Fredrikson, 1990, 1991). The *Polygonum* type of embryo sac is the most common in flowering plants and is considered as a primitive embryological features, while the *Allium* (e.g. *Cymbidium bicolor*; Swamy, 1942a) and the *Adoxa* (e.g. *Epipactis pubescens*; Brown & Sharp, 1911) types are considered to be derived. The *Allium* type is more common than the *Adoxa* type (Li et al., 2003).

From our observation, it is clear that the pollen tube penetrates the embryo sac through the micropyle (porogamy), which is found in the majority of angiosperms (Maheshwari, 1950).

Swamy (1949b) categorized orchid embryos into the three groups namely group A (Asterad type), group B (Onagrad type) and group C (Cymbidium type). In group A, the suspensor initial cell (*ci*), middle cell (*m*), and terminal cell (*ca*) take part in the formation of the mature embryo, whereas in group B the suspensor initial cell gives rise to the suspensor while the mature embryo is established from the derivatives of the terminal and middle cells only. In group C the divisions in the basal and terminal cells of the two-celled proembryo are irregular. In this study of *S. plicata* the mature embryo was formed by the derivatives of the terminal and middle cells, and so the embryological developmental pattern of *S. plicata* belongs to the group B or *Onagrad* type. This embryological type corresponds to the Cypripedioid type (plesiomorphic type) of Clements (1999), and is found in a number of orchid groups that have traditionally been placed in separate subfamilies.

In a previous report (Raghavan & Goh, 1994), as well as in this present investigation, the embryo of *S. plicata* was found to contain different sized cells with the proximal end consisting of smaller cells that occupy 1/3 of the body of mature embryo. A similar observation has also been reported in *Vanda* sp. (Raghavan, 1997) and *Phalaenopsis amabilis* var. *formosa* (Lee et al., 2008). Batygina et al. (2003) and Lee et al. (2013) suggested that the size of small-celled part of the embryo both depends on the stage of embryo development and is taxon-specific.

TABLE 2. Comparative embryological characters in two species of *Spathoglottis*.

Species	Triad	T-tetrad megaspores	Linear tetrad megaspores	Duration between pollination and fertilization
S. plicata (Swamy, 1949a, b)	-	+	-	15 d
S. plicata (current study)	-	-	+	15 d
S. affinis (Sriyot et al.; unpub. data)	+	-	-	21 d

+ = present, - = absent (Both species were monosporic in the three studies)

Based on the suspensor morphology, Swamy (1949b) classified the suspensor within the Orchidaceae into the five types of: (1) unicellular, enlarged to become sac-like, conical or tubular form (*Cirrhopetalum fimbriatum*; Ekanthappa & Arekal, 1977); (2) uniseriate filament of five to ten cells growing beyond the micropyle (*Habenaria* spp.; Swamy, 1946; Sood, 1986); (3) appears as a group of grapes (*Sobralia*, *Epidendrum*; Swamy, 1943a); (4) the suspensor divides by three vertical divisions, and the eight cells thus formed elongate downwards surrounding more than half of the embryo (*Vanda* spp.; Swamy, 1942b); and (5) at the four cells suspensor stage, two cells lead towards the micropylar end and the other two direct to the chalazal end, elongate and form tubular structures (*Eulophia andamanensis*; Sriyot & Thammathaworn, 2010). Swamy (1943a, 1949b) and Veyret (1974) reported that the suspensor of *S. plicata* is of tubular form, one-celled and elongated towards the micropylar end. In contrast, our investigation showed sac-like, cap-like or globular forms with a hypertrophied nucleus (Fig. 8B–D). A unicellular suspensor has also been observed in *Spathoglottis aurea* (Chua & Rao, 1978); *Microstylis cylindrostachya* (Sood, 1985) and *Malaxis saprophyta* (Sood, 1992).

Polyembryony among Orchidaceae is predominantly due to cleavage polyembryony, and this type of polyembryony has already been reported in many taxa (Swamy, 1946; Chua & Rao, 1978). Swamy (1943b) noted three different modes in which cleavage polyembryony in orchids is formed; (1) the zygote divides irregularly to form a mass of cells, of which those lying towards the chalazal end grow simultaneously and give rise to many embryos; (2) the filamentous embryo becomes branched and each of the branches gives rise to an independent embryo; and (3) the proembryo gives out small buds or outgrowths which may themselves function as embryos. Moreover, an especially interesting type of cleavage polyembryony originates in *Cymbidium bicolor* (Swamy, 1942a), where the resulting seeds contain two embryos each, one of them being slightly smaller. Although a polyembryonic condition was not detected in the early stages of embryo development in this study,

considering the number and size of the embryos, it seems that polyembryony in *S. plicata* is due to cleavage, and in particular is of the *Cymbidium* type. One of the twin embryos is slightly smaller than the other, probably due to competition for space or nutrition and its tardy development as compared with its counterpart (Swamy, 1942a; Ansari, 1977).

Embryological characters can be used to support taxonomic distinction at the familial and generic levels (Maheshwari, 1950; Johri et al., 1992) and the information for *S. plicata* and the related *S. affinis* summarized in Table 2 supports this statement. For example, although these two closely related species of *Spathoglottis* have a monosporic pattern of embryo sac development, a difference was found in the patterns of megaspores, where *S. plicata* possesses T-tetrad and/or linear megaspores, and *S. affinis* possesses the triad type. The occurrence of triads in Orchidaceae is twice as common as tetrads (Savina, 1978).

In the Orchidaceae, the duration between pollination and fertilization is highly variable (Swamy, 1943a), but is usually short in terrestrial orchids in the subfamily Spiranthoideae and Orchidoideae (Swamy, 1949b). The shortest period so far noted is 4 d in *Gastrodia elata* and the longest is in *Vanda suavis* (Swamy, 1943a). In *Habenaria*, it takes 8–10 d (Swamy, 1946), whereas this duration varies from 5 d to 3 months in the Epidendroid taxa, such as 54 d in *Eulophia andamanensis* (Sriyot & Thammathaworn, 2010) and 60 d in *Geodorum densiflorum* and *Bulbophyllum mysorense* (Swamy, 1949b), while it takes 15 d in *S. plicata* (Table 2). Each orchid species, therefore, appears to have stabilized its time interval for different developmental stages in relation to the environment and the availability of species-specific pollinators (Attri et al., 2012).

Characteristics of the outer periclinal and anticlinal cell walls of the testa cells could be useful at higher taxonomic ranks (subtribal and tribal level). However, considering the large number of genera and species in Orchidaceae, a comparative study of seed micromorphology in other species is needed to compare these characters and to clarify their role in taxonomy and phylogeny (Dressler, 1993; Molvray & Chase, 1999).

ACKNOWLEDGEMENTS

The authors express their indebtedness to Assoc. Prof. Dr. Johanna Wagner for her valuable suggestions and providing all the facilities while the first author was working at the Institute of Botany, Faculty of Biology, University of Innsbruck, Austria. We thank Mr. Werner Kofler who introduced the first author to SEM. This research was funded by the Science Achievement Scholarship of Thailand and the Salt-tolerant Rice Research Group, Khon Kaen University.

LITERATURE CITED

Aewsakul, N., Maneesorn, D., Serivichyaswat, P., Taluengjit, A. and Nontachaiyapoom, S. 2013. *Ex vitro* Symbiotic Seed Germination of *Spathoglottis plicata* Blume on Common Orchid Cultivation Substrates. Scientia Horticulturae, 160: 238-242.

Ansari, R. 1977. Observations on the Occurrence of Polyembryony in Two Species of Orchids. Current Science, 46: 607.

Attri, L.K., Nayyar, H. and Kant, R. 2012. Embryological Studies in Orchids: An Observation on *Cymbidium pendulum* (Roxb.) Sw. Indian Journal of Fundamental and Applied Life Sciences, 2: 8-13.

Aybeke, M. 2012. Anther Wall and Pollen Development in *Ophrys manmosa* L. (Orchidaceae). Plant Systematics and Evolution, 298: 1015-1023.

Batygina, T.B., Bragina, E.A. and Vasilyeva, V.E. 2003. The Reproductive System and Germination in Orchids. Acta Biologica Cracoviensia Series Botanica, 45: 21-34.

Beltrame, E. 2006. *Spathoglottis*-Inside and Out. Orchid Review, 114: 68-71.

Bhanwra, R.K, Vij, S.P., Kant, R., Chandel, V. and Dutt, S. 2006. Pollinium Development in *Epipactis veratrifolia* Boiss and Hohen. Journal of Orchid Society of India, 20: 1-6.

Brown, W.H. and Sharp, L.W. 1911. The Embryo Sac of *Epipactis*. Botanical Gazette, 52: 439-452.

Chua, L.G. and Rao, A.N. 1978. Polyembryony and Suspensor Characteristics in *Spathoglottis*. Flora (Jena), 167: 399-402.

Clements, M.A. 1999. Embryology. In: Pridgeon, A.M., Cribb, P.J., Chase, M.W. and Rasmussen, F.N. (Eds.). Genera Orchidacearum Volume 1 General Introduction, Apostasioideae, Cypripedioideae, Oxford University Press Inc., New York, 38-58 pp.

Dafni, A. and Maués, M.M. 1998. A Rapid and Simple Procedure to Determine Stigma Receptivity. Sexual Plant Reproduction, 11: 177-180.

Dressler, R.L. 1993. Phylogeny and Classification of the Orchid Family, Cambridge University Press, UK, 314 pp.

Ekanthappa, K.G. and Arekal, G.D. 1977. A Contribution to the Embryology of *Cirrhopetalum fimbriatum* Lindl. Proceedings of the Indian Academy of Sciences, 86 B: 211-216.

Fredrikson, M. 1990. Embryological Study of *Herminium monorchis* (Orchidaceae) Using Confocal Scanning Laser Microscopy. American Journal of Botany, 77: 123-127.

Fredrikson, M. 1991. An Embryological Study of *Platanthera bifolia* (Orchidaceae). Plant Systematics and Evolution, 174: 213-220.

Freudenstein, J.V. and Rasmussen, F.N. 1996. Pollinium Development and Number in the Orchidaceae. American Journal of Botany, 83: 813-824.

Herr, J.M., Jr. 1971. A New Clearing-Squash Technique for the Study of Ovule Development in Angiosperms. American Journal of Botany, 58: 785-790.

Johri, B.M., Ambegaokar, K.B. and Srivastava, P.S. 1992. Comparative Embryology of Angiosperms Vol. 2, Springer-Verlag, Germany, 1,221 pp.

Kant, R. and Bhanwra, R.K. 2010. Development of Anther in Relation to Sectile Pollinium in *Zeuxine strateumatica* (Lindl.) Schltr. Journal of Biology and Life Sciences, 1: 5-12.

Kant, R., Hossain, M.M. and Attri, L.K. 2013. Pollinium Development in *Spiranthes sinensis* (Pers.) Ames. and *Cymbidium pendulum* Sw: A Comparative Study. Bangladesh Journal of Botany, 42: 307-314.

Kauth, P.J., Johnson, T.R., Stewart, S.L. and Kane, M.E. 2008. A Classroom Exercise in Hand Pollination and *in vitro* Asymbiotic Orchid Seed Germination. Plant Cell, Tissue and Organ Culture, 93: 223-230.

Kheawwongjun, J. and Thammasiri**,** K. 2008. Breeding *Spathoglottis* spp. for Commercial Potted Orchids. Acta Horticulturae, 788: 47-52.

Lee, Y.-I., Hsu, S.-T. and Yeung, E.C. 2013. Orchid Protocorm-Like Bodies are Somatic Embryos. American Journal of Botany, 100: 2121-2131.

Lee, Y.-I., Yeung, E.C., Lee, N. and Chung, M.-C. 2008. Embryology of *Phalaenopsis amabilis* var. *formosa*: Embryo Development. Botanical Studies, 49: 139-146.

Li, L., Liang, H.-X., Peng, H. and Lei, L.-G. 2003. Sporogenesis and Gametogenesis in *Sladenia* and Their Systematic Implication. Botanical Journal of the Linnean Society**,** 143: 305-314.

Maheshwari, P. 1950. An Introduction to the Embryology of Angiosperms, Tata McGraw-Hill, New Delhi, 453 pp.

Minea, M., Piluek, C., Menakanit, A. and Tantiwiwat, S. 2004. A Study on Seed Germination and Seedling Development of *Spathoglottis* Bl. Orchids. Kasetsart Journal (Natural Science), 38:141-156.

Molvray, M. and Chase, M.W. 1999. Seed Morphology. In: Pridgeon, A.M., Cribb, P.J., Chase, M.W. and Rasmussen, F.N. (Eds.). Genera Orchidacearum Volume 1 General Introduction, Apostasioideae, Cypripedioideae, Oxford University Press Inc., New York, 59-66 pp.

Novak, S.D. and Whitehouse, G.A. 2013. Auxin Regulates First Leaf Development and Promotes the Formation of Protocorm Trichomes and Rhizome-Like Structures in Developing Seedlings of *Spathoglottis plicata* (Orchidaceae). AoB Plants, 5: pls053. doi:10.1093/aobpla/pls053.

Prakash, N. and Lee-Lee, A. 1973. Life History of a Common Malaysian Orchid *Spathoglottis plicata*. Phytomorphology, 23: 9-17.

Pridgeon, A.M. 1999. Palynology. In: Pridgeon, A.M., Cribb, P.J., Chase, M.W. and Rasmussen, F.N. (Eds.). Genera Orchidacearum Volume 1 General Introduction, Apostasioideae, Cypripedioideae, Oxford University Press Inc., New York, 33-37 pp.

Punt, W., Hoen, P.P., Blackmore, S., Nilsson, S. and Le Thomas, A. 2007. Glossary of Pollen and Spore Terminology. Review of Palaeobotany and Palynology, 143: 1-81.

Raghavan, V. 1997. Molecular Embryology of Flowering Plants, Cambridge University Press, New York, 690 pp.

Raghavan, V. and Goh, C.J. 1994. DNA Synthesis and mRNA Accumulation During Germination of Embryos of the Orchid *Spathoglottis plicata*. Protoplasma, 183: 137-147.

Ramesh, T. and Ranganathan, P. 2008. Cytological Studies on Some Commercial Orchids. Plant Archives, 8: 139-141.

Savina, G.I. 1978. Certain Peculiarities in the Embryology of Orchids. Proceedings of the Indian National Science Academy, B 44: 141-145.

Sebastinraj, J. and Muhirkuzhali, S. 2014. Asymbiotic Seed Germination and Micropropagation of *Spathoglottis plicata* Blume. International Journal of Advances in Pharmacy, Biology and Chemistry, 3: 495-501.

Seidenfaden, G. 1986. Orchid Genera in Thailand XIII. Thirty-Three Epidendroid Genera. Opera Botanica, 89: 1-214.

Seidenfaden, G. and Wood, J.J. 1992. The Orchids of Peninsular Malaysia and Singapore, Olsen & Olsen, Fredensborg, Denmark, 779 pp.

Sinha, P., Hakim, M.L. and Alam, M.F. 2009. *In vitro* Mass Clonal Propagation of *Spathoglottis plicata* Blume. Plant Tissue Culture and Biotechnology, 19: 151-160.

Soguillon, S. and Rosario, T.L. 2007. Developmental Characterization of Pods of Ground Orchid *Spathoglottis plicata* 'Alba'. Philippine Journal of Crop Science, 32: 109-117.

Sood, S.K. 1985. Gametophytes, Integuments Initiation and Embryogeny in *Microstylis cylindrostachya* (Orchidaceae, Epidendreae). Proceedings of the Indian Academy of Sciences (Plant Science), 95: 379-387.

Sood, S.K. 1986. Gametogenesis, Integuments Initiation and Embryogeny in Three Species of *Habenaria* (Orchidaceae, Orchideae). Proceedings of the Indian Academy of Sciences (Plant Science), 96: 487-494.

Sood, S.K. 1992. Embryology of *Malaxis saprophyta*, with Comments on the Systematic Position of *Malaxis* (Orchidaceae). Plant Systematics and Evolution, 179: 95-105.

Sood, S.K. 1997. Gametogenesis, Seed Development and Pericarp in *Epipactis latifolia* (Orchidaceae, Neottieae). Journal of the Indian Botanical Society, 76: 11-15.

Sood, S.K. and Rao, P.R.M. 1988. Studies in the Embryology of the Diandrous Orchid *Cypripedium cordigerum* (Cypripedieae, Orchidaceae). Plant Systematics and Evolution, 160: 159-168.

Sriyot, N. and Thammathaworn, A. 2010. Sporogenesis, Gametogenesis and Embryogenesis of *Eulophia andamanensis* Rchb.f. Thai Journal of Botany, 2: 83-99. (in Thai)

Stelly, D.M., Peloquin, S.J., Palmer, R.G. and Crane, C.F. 1984. Mayer's Hamalum-Methyl Salicylate: A Stain Clearing Technique for Observations within Whole Ovules. Stain Technology, 59: 155-161.

Swamy, B.G.L. 1942a. Female Gametophyte and Embryogeny in *Cymbidium bicolor* Lindl. Proceedings of the Indian Academy of Sciences**,** 15: 194-201.

Swamy, B.G.L. 1942b. Morphological Studies in Three Species of *Vanda*. Current Science, 11: 285-286.

Swamy, B.G.L. 1943a. Embryology of Orchidaceae. Current Science, 12: 13-17.

Swamy, B.G.L. 1943b. Gametogenesis and Embryogeny of *Eulophia epidendraea* Fischer. Proceedings of the National Institute of Sciences of India Part B, 9: 59-65.

Swamy, B.G.L. 1946. Embryology of *Habenaria*. Proceedings of the National Institute of Sciences of India Part B, 12: 413-426.

Swamy, B.G.L. 1949a. Embryological Studies in the Orchidaceae. I. Gametophyte. American Midland Naturalist, 41: 184-201.

Swamy, B.G.L. 1949b. Embryological Studies in the Orchidaceae. II. Embryogeny. American Midland Naturalist, 41: 202-232.

Teng, W.L., Nicholson, L. and Teng, M.C. 1997. Micropropagation of *Spathoglottis plicata*. Plant Cell Reports, 16: 831-835.

Thakur, U. and Dongarwar, N. 2012. Artificial Pollination and *in vitro* Asymbiotic Seed Germination in Garden Orchid *Spathoglottis*

plicata Blume (Orchidaceae). Recent Research in Science and Technology, 4: 13-18.

Thammathaworn, A. 1995. Handbook for Micro-technique in Biology, Department of Biology, Faculty of Science, Khon Kaen University, Thailand, 21 pp. (in Thai)

Veyret, Y. 1974. Development of the Embryo and the Young Seedling Stages of Orchids. In: Withner C.L. (Ed.). The Orchids: Scientific Studies. John Wiley & Sons Inc., New York, 223-265 pp.

Wang, X.-J., Loh, C.-S., Yeoh, H.-H. and Sun, W.Q. 2002. Drying Rate and Dehydrin Synthesis Associated with Abscisic Acid-Induced Dehydration Tolerance in *Spathoglottis plicata* Orchidaceae Protocorms. Journal of Experimental Botany, 53: 551-558.

Wang, X.-J., Loh, C.-S., Yeoh, H.-H. and Sun, W.Q. 2003. Differential Mechanisms to Induce Dehydration Tolerance by Abscisic Acid and Sucrose in *Spathoglottis plicata* (Orchidaceae) Protocorms. Plant, Cell and Environment, 26: 737-744.

Yang, M. and Loh, C.S. 2004. Systemic Endopoly-ploidy in *Spathoglottis plicata* (Orchidaceae) Development. BMC Cell Biology, 5: 33. doi:10.1186/1471-2121-5-33.